Addressing some artifacts in PP-PS registration prior to performing joint impedance inversion

Satinder Chopra and Ritesh Kumar Sharma*
TGS, Calgary

Summary

Multicomponent seismic data analysis enhances confidence in interpretation as it provides the mode-converted PS data for imaging of the subsurface. The integrated interpretation of PP and PS data begins with the identification of reflections corresponding to similar geologic events on both datasets. This identification is accomplished by carrying out well log correlation through the generation of PP and PS synthetic seismograms. Though it may seem to be a straightforward approach there are a few issues associated with it. One of them is the lower resolution of the PS data than the PP data which presents difficulties in the correlation of the equivalent reflection events on both the datasets. Even if few consistent horizons get tracked, the horizon matching process introduces some artifacts on the PS data mapped into PP time. In this exercise, we elaborate on such challenges with a dataset from the Anadarko Basin in the US, and then propose a novel workflow for addressing them.

Introduction

The integrated interpretation of PP and PS data begins with the identification of reflections corresponding to similar geologic events on both datasets. The identification is accomplished by carrying out well log correlation through the generation of PP and PS synthetic seismograms. If check shots or VSP data are not available, slight stretching/squeezing may be necessary. One way to generate a PS synthetic seismogram is to use V_S and density curves to generate a PS elastic gather with a wavelet extracted from PS stacked data and stack it. The stacked gather trace can be correlated with the PS stacked data. The other method is to generate the angle-dependent PS reflectivity at 10 or 12 degrees and use it for generating the PS synthetic seismogram. It is assumed here that a shear sonic curve is available and both synthetic seismograms are generated over the same range of frequency bandwidth as the input seismic reflection data.

Such a correlation helps with the visual identification of events on PS section at the location of the well, considering their character, relative amplitudes as well as their approximate travel times. In a similar way, reflection events are identified on the PP data. When the events of interest are identified and correlated on both the PP and PS sections (through the respective synthetic seismograms) at the location of the wells, horizons are picked on the data volumes on an interpretation workstation. The polarity convention adopted is the peak on the PP and PS data represent an increase in elastic impedance across the interface it is representing. Mis-ties may be seen on such synthetic-seismic correlations and one should keep an open mind while analyzing the reasons for the same.

While doing event correlations between the PP and PS data, a peak on PP data is expected to correlate with an equivalent peak on the PS data. Sometimes, this is not found to be the case. A familiar example to cite is from the oil sands area in northern Alberta, Canada, where the Paleozoic marker is a difficult pick. The Paleozoic marker is a weathered unconformity between the Paleozoic carbonates and Cretaceous clastics. The relative compressibility and rigidity of the weathered carbonates as well as the tuning artifacts make the seismic response exhibit a peak at places, then becomes a zero crossing or a trough. (Anderson and Larson, 2006). In such cases, a prominent horizon above or below can be used for horizon picking.

Next, the equivalent correlative events on the PP and PS data volumes are used to map or shrink the PS time scale to the PP time scale, a process referred to as *registration*. This step entails complications varying from difficulty in picking horizons in areas with complicated geology entailing faulting, etc., one or more peaks on PP data corresponding to a trough on PS data, and the frequency content of PS data being much lower than that of PP data due to different attenuations suffered by component frequencies during wave propagation. Some automated methods based on warping of one dataset with the other have been introduced (Herrera and van der Baan, 2012, Hale, 2013; Compton and Hale, 2014, Gao and Sacchi, 2018), but in the absence of adequate software for such methods, the above-mentioned manual registration exercise can be resorted to. Excessive care is required in performing this step as any artifact(s) introduced here will show up on the joint impedance inversion as well as lead to incorrect interpretation. We emphasize the above artifacts as applicable to a dataset from the Anadarko Basin in Oklahoma, US and present a workflow for addressing them.

Artifacts resulting from the application of conventional workflow

As stated above, once the well-to-seismic correlation for PP and PS seismic data are done satisfactorily, horizon picking is carried out to map all trackable horizons on PS data that are equivalent to those picked on PP data. The depth-time curves for both PP and PS data are determined at the well location to estimate V_P/V_S in different intervals. The estimated interval V_P/V_S at the well is propagated over the 3D seismic data to obtain an initial V_P/V_S volume, that is used to transform PS data from its original time domain to PP time domain. Had it been valid everywhere, a perfect match between PP and PS horizons would have been noticed. However, a mismatch between the two types of horizons, except at the well location is generally noticed as shown in Figure 1a and b. Geologically though, such a mismatch is not acceptable, as a geological marker would be expected at the same time on both the datasets after registration. The discrepancies show up as the interval V_P/V_S is only valid at the well location and may not be valid at other lateral locations.

We try and match the picked horizons on both PP and PS data so as to make them geologically consistent. The residual V_P/V_S values used in the domain conversion can be estimated by using the PP and PS isochrons in the following equation (Garotta, et al., 1985).

$$\frac{V_P}{V_S} = 2\left(\frac{PS\ isochron}{PP\ isochron}\right) - 1. \qquad (1)$$

10.1190/segam2019-w6-04.1

The V_P/V_S values so computed at every trace are compared with the initial V_P/V_S volume. The observed differences (in V_P/V_S) are spread out within the intervals at every CMP location, resulting in time shifts of reflection events.

While this process solves the horizon mismatch problem at the boundaries of various intervals bounded by horizons, some artifacts are seen within the intervals as shown in Figure 1c, that shows an equivalent PS section in PP time with V_P/V_S overlay. The revised values are again shown in color which exhibits an uneven distribution. Besides this, some of the reflections are also seen as having undulations as indicated within the cyan ellipse to the right side of Figure 1c. One could attempt skipping the matching of the Meramec horizons in-between the Big Lime and Woodford markers, which tends to distribute the V_P/V_S values better as shown in Figure 1d. The jitter in the seismic reflections indicated within the cyan ellipse in Figure 1c is also minimized. Thus, it seems the problem is alleviated though of course, this may not happen every time skipping of an intermediate horizon is attempted. We consider such observations as artifacts, which if not corrected properly before performing prestack joint impedance inversion could degrade the results.

Besides this important issue, the other issue has to do with the significant difference in the PP and PS spectral bandwidth after registration. This is found to be generally true and again results in the degradation of the prestack joint inversion performance.

Attempts at addressing the artifacts

A workflow has been put together for addressing the above-mentioned artifacts and is shown in Figure 2. After performing the well-to-seismic correlations for both PP and PS seismic data, and using the picked horizons bounding the broad zone of interest, the PS data are transformed into PP two-way travel time. As the next step, the frequency spectra balancing of the PS data is taken up. The method adopted for spectral flattening by balancing the power (square of the spectral magnitude) was first discussed by Marfurt and Matos (2014) and makes use of the average power spectrum at a given time as well as the average spectral magnitude. As a single time-varying spectral balancing operator is applied to every trace, this spectral balancing approach is considered amplitude-friendly (Chopra and Marfurt, 2016). As both the PP and PS data could have different amplitude levels, the next step normalizes the two datasets using a z-transformation, requiring the computation of the mean and standard deviation. Thereafter, using the picked horizons, stratal intervals are defined over the broad zone of interest on both PP and PS data, and crosscorrelated to find time shifts for maximum correlation. Such time shifts are linearly interpolated to produce a volume of time shifts that would align PP and PS seismic data.

In Figure 3a we exhibit an S-impedance section obtained from prestack joint impedance inversion, before using the proposed workflow and the equivalent section after using it is shown in Figure 3b. Notice the clearer definition of the event marked with the cyan arrow to the right, after following the proposed workflow.

Similarly, in Figure 4 we show V_P/V_S equivalent arbitrary-line sections drawn from V_P/V_S volumes obtained by using prestack joint impedance inversion, before and after using the proposed workflow. Notice the overall better resolution seen in Figure 4b.

We take this analysis forward and in Figure 5 show the comparison of the crossplots between P-impedance and V_P/V_S generated from well data (Figure 5a), as well as the inverted data, before (Figure 5b) and after using the proposed workflow (Figure 5c). Not only are the overall clusters of inverted data following the trend seen for the well data, but the cluster points corresponding to low-V_P/V_S and low-impedance separate out better after balancing as shown in the highlighting ellipses. Such a separation has an important implication in that when such cluster points are back projected on the vertical seismic sections, they illuminate the sweet spots better.

Conclusions

In this study, attention has been drawn to a couple of important issues that crop up while performing registration of multicomponent PS and PP seismic data before the data are taken into prestack joint impedance inversion. These issues are the generation of uneven or abnormal V_P/V_S values in the different intervals as well as the lower frequency content of PS data after domain conversion to PP two-way travel time. If such issues are left unaddressed, they lead to artifacts in the prestack joint impedance inversion carried out for generation of elastic parameters. We have devised a workflow that addresses the above issues and produces results that are free from artifacts leading to superior and more meaningful results.

Acknowledgements

We wish to thank TGS for encouraging this work and for the permission to present and publish it. The well data used in this work was obtained from the TGS Well Data Library and is gratefully acknowledged.

10.1190/segam2019-w6-04.1

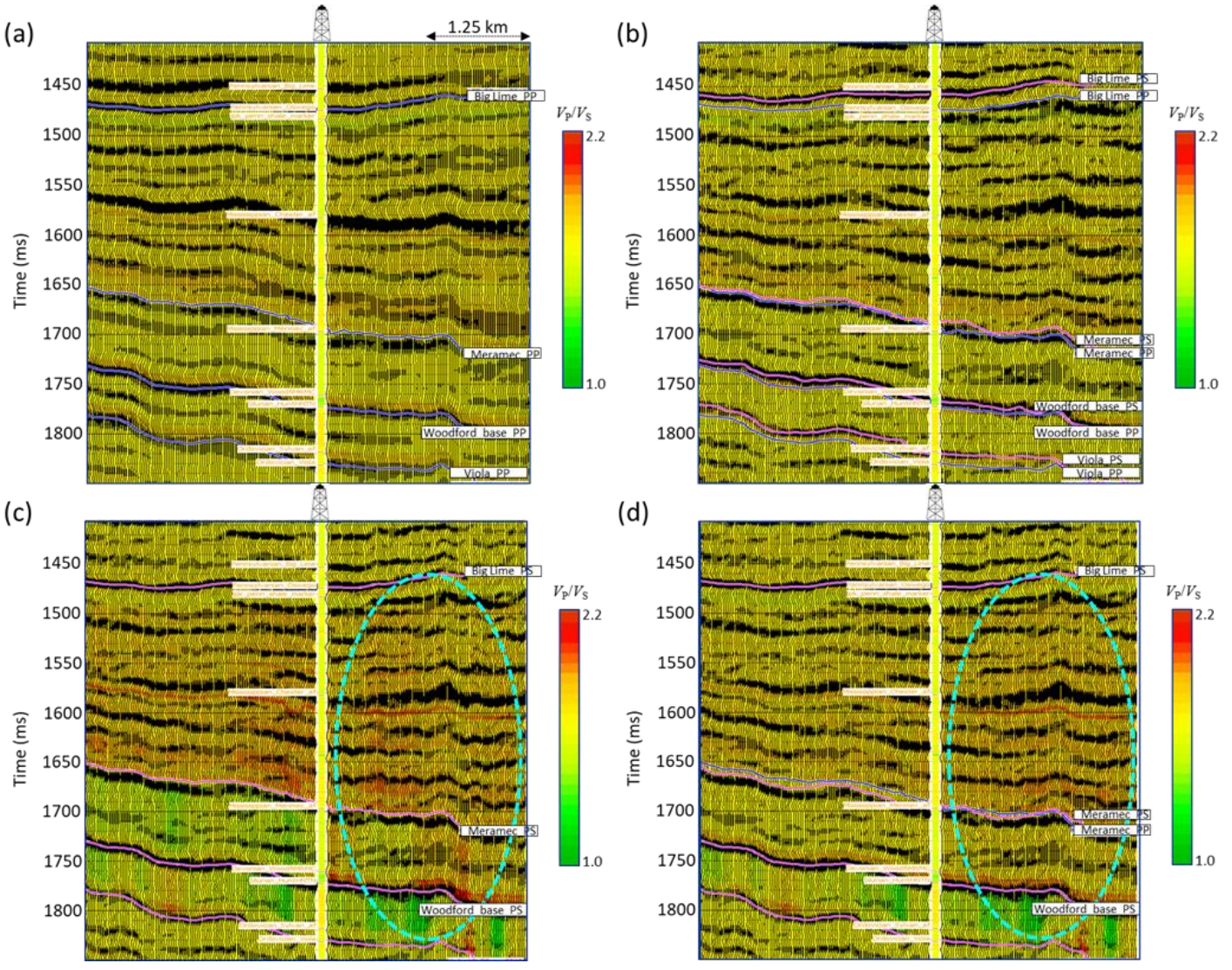

Figure 1: Segments of seismic sections from (a) PP and (b) PS data in PP time. Four equivalent reflection events have been picked on the data volumes separately as pointed out by the coloured block arrows to the right, but horizon matching has not been done yet. The V_P/V_S values at every CDP are overlaid in colour. (c) The same PS section as in (b) but with horizons matched. Notice the revised values of V_P/V_S which seem uneven in red and green and not correlated with the well log curve so well. Also notice the reflection distortions in the form of undulations within the cyan ellipse to the right. (d) The same section as in (c) but skipping the matching of the Meramec horizons during horizon matching. The distortion in the reflections is minimized and the V_P/V_S values seem to be spread out better. (*Data courtesy of TGS, Houston*)

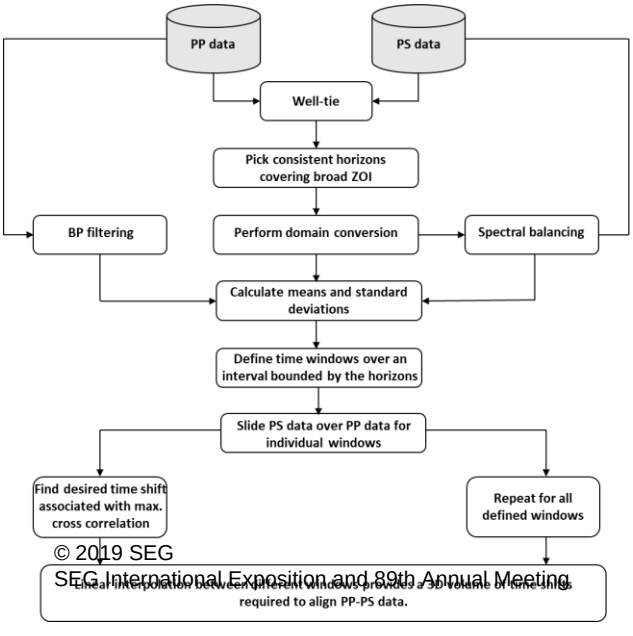

Figure 2: Block diagram explaining the proposed workflow.

10.1190/segam2019-w6-04.1

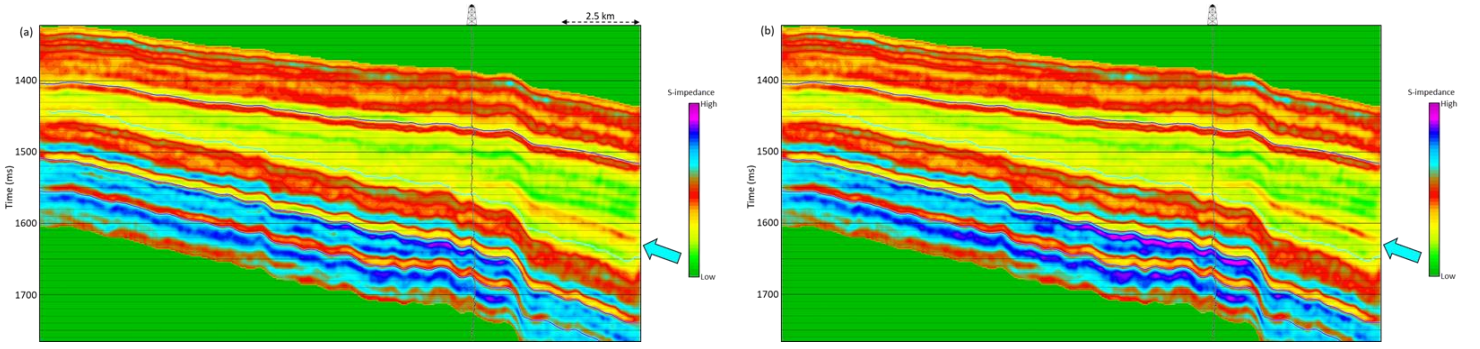

Figure 3: Segments of S-impedance sections obtained from prestack joint impedance inversion (a) before, and (b) after spectral balancing of the PS seismic data (in PP time). Notice the stronger definition of the event pointed at by the cyan arrow to the right. (*Data courtesy of TGS, Houston*)

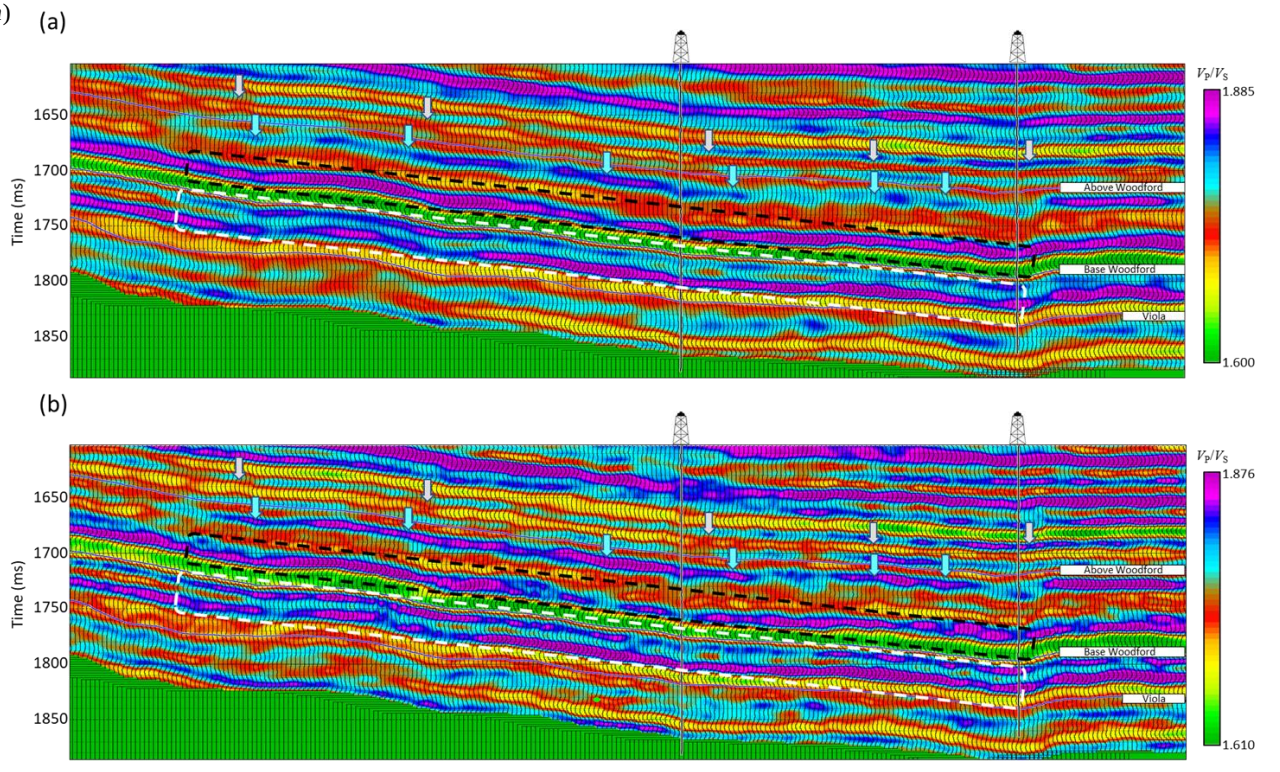

Figure 4: An arbitrary line passing through two wells from the V_P/V_S volume generated using pre-stack joint impedance inversion (a) before, and (b) after balancing. Notice the overall better resolution seen in the different intervals after spectral balancing. (*Data courtesy of TGS, Houston*)

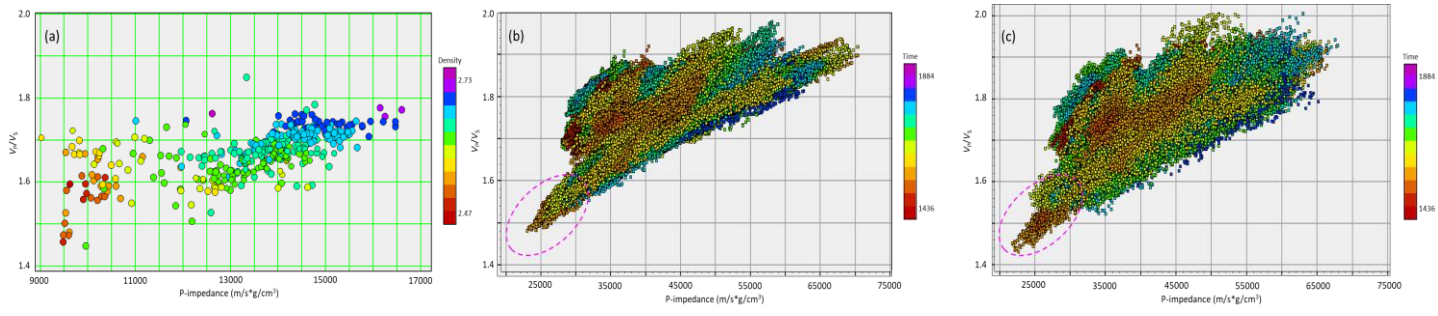

Figure 5: Crossplot between P-impedance and V_P/V_S colour-coded with density from well data between the Meramec and base of Woodford interval. Equivalent crossplots generated using prestack joint inversion, (b) before and (c) after spectral balancing, colour-coded with time for the same interval. Not only is the overall cluster of inverted data following the trend seen for the well data, but the cluster points corresponding to low-V_P/V_S and low-impedance separate out after balancing as shown in the highlighting ellipse. (*Data courtesy of TGS, Houston*)

10.1190/segam2019-w6-04.1

REFERENCES

Anderson, P., and R., Larson, 2006, Multicomponent case study: One company's experience in eastern Alberta: CSEG Recorder, **31**, no. 9, 5–10.

Chopra, S., and K. J., Marfurt, 2016, Spectral decomposition and spectral balancing of seismic data: The Leading Edge, **35**, no. 2, 176–179, doi: https://doi.org/10.1190/tle35020176.1.

Compton, S., and D., Hale, 2014, Estimating VP/VS ratios using smooth dynamic image warping: Geophysics, **79**, no. 6, V201–V215, doi: https://doi.org/10.1190/geo2014-0022.1.

Gao, W., and M. D., Sacchi, 2018, Multicomponent seismic data registration by nonlinear optimization: Geophysics, **83**, no. 1, V1–V10, doi: https://doi.org/10.1190/geo2017-0105.1.

Garotta, R., P., Marechal, and M., Mehesan, 1985, Two-component acquisition as a routine procedure for recording P-waves and converted waves: Canadian Journal of Exploration Geophysics, **21**, 40–53.

Hale, D., 2013, Dynamic warping of seismic images: Geophysics, **78**, no. 2, S105–S115, doi: https://doi.org/10.1190/geo2012-0327.1.

Herrera, R. H., and M., van der Baan, 2012, Guided seismic-to-well tying based on dynamic time warping: 82nd Annual International Meeting, SEG, Expanded Abstracts, 1–5, doi: https://doi.org/10.1190/segam2012-0712.1.

Marfurt, K., and M., Matos, 2014, Am I blue? Finding the right (spectral) balance: AAPG Explorer, https://doi.org/http://www.aapg.org/publicatiohttps://doi.org/ns/news/explorer/column/articleid/9522/am-i-blue-finding-the-right-spectral-balance, accessed 12 March 2015.